





Center of mass and anatomical coordinate system definition for sheep head kinematics, with application to ovine models of traumatic brain injury

Jessica M. Sharkey¹  | Ryan D. Quarrington²  | Charlie C. Magarey^{2,3}  |
Claire F. Jones^{2,3} 

¹Translational Neuropathology Laboratory, School of Biomedicine, The University of Adelaide, Adelaide, South Australia, Australia

²Adelaide Spinal Research Group, Centre for Orthopaedic & Trauma Research, Adelaide Medical School, The University of Adelaide, Adelaide, South Australia, Australia

³School of Mechanical Engineering, The University of Adelaide, Adelaide, South Australia, Australia

Correspondence

Claire F. Jones, School of Mechanical Engineering and Centre for Orthopaedic & Trauma Research, Adelaide Medical School, The University of Adelaide, Adelaide, SA 5005, Australia.
Email: claire.jones@adelaide.edu.au

Abstract

Pathological outcomes of traumatic brain injury (TBI), including diffuse axonal injury, are influenced by the direction, magnitude, and duration of head acceleration during the injury exposure. Ovine models have been used to study injury mechanics and pathological outcomes of TBI. To accurately describe the kinematics of the head during an injury exposure, and better facilitate comparison with human head kinematics, anatomical coordinate systems (ACS) with an origin at the head or brain center of mass (CoM), and axes that align with the ovine Frankfort plane equivalent, are required. The aim of this study was to determine the mass properties of the sheep head and brain, and define an ACS_{virtual} for the head and brain, using anatomical landmarks on the skull with the aforementioned origins and orientation. Three-dimensional models of 10 merino sheep heads were constructed from computed tomography images, and the coordinates of the head and brain CoMs, relative to a previously reported sheep head coordinate system (ACS_{physical}), were determined using the Hounsfield unit–mass density relationship. The ACS_{physical} origin was 34.8 ± 3.1 mm posterosuperior of the head CoM and 43.7 ± 1.7 mm anteroinferior of the brain CoM. Prominent internal anatomical landmarks were then used to define a new ACS (ACS_{virtual}) with axes aligned with the Frankfort plane equivalent and an origin 10.4 ± 3.2 mm from the head CoM. The CoM and ACS_{virtual} defined in this study will increase the potential for comparison of head kinematics between ovine models and humans, in the context of TBI.

KEYWORDS

anatomical coordinate system, brain, center of mass, ovine, preclinical model, skull, traumatic brain injury

Jessica M. Sharkey and Ryan D. Quarrington joint first author.
Reviewed by Ricardo Secoli, Matthieu Keller and Robert Anderson

This is an open access article under the terms of the [Creative Commons Attribution-NonCommercial-NoDerivs](https://creativecommons.org/licenses/by-nc-nd/4.0/) License, which permits use and distribution in any medium, provided the original work is properly cited, the use is non-commercial and no modifications or adaptations are made.

© 2022 The Authors. *Journal of Neuroscience Research* published by Wiley Periodicals LLC.

1 | INTRODUCTION

Traumatic brain injury (TBI) is the leading cause of death and disability in people aged under 45 years (Popescu et al., 2015). Despite 69 million people worldwide sustaining TBI every year, this life-threatening injury is still poorly understood (Dewan et al., 2019). A key cause of neurological impairment following TBI is damage to the axonal white matter tracts in the brain (Smith et al., 2003). Diffuse axonal injury (DAI) is present in mild, moderate, and severe TBI and increases with worsening injury severity (Smith et al., 2003). The precise mechanisms and tolerance criteria for the development of DAI are not currently known (Meaney et al., 2014).

Animal models, cadaver models, injury reconstructions, and finite element (FE) models, have been used to investigate brain tissue mechanical and/or pathological response to closed-head injury exposures (e.g., Alshareef et al., 2020; McIntosh et al., 2014; Namjoshi et al., 2013; Ueno & Melvin, 1995). Where head motion is allowed in animal models, acceleration due to an applied force (either impact or inertial) can produce focal and diffuse brain tissue damage (Anderson et al., 2003; Gennarelli et al., 1982; Lewis et al., 1996; Smith et al., 1997). When the applied force is aligned with the center of mass (CoM) of the head, linear acceleration is produced, whereas a force that is applied eccentrically to the CoM of the head causes rotational acceleration (Zuckerman et al., 2018). Linear head kinematics during TBI events are typically associated with focal hematomas and contusions, while rotational kinematics are thought to predominantly produce DAI pathology (Holbourn, 1943; Kleiven, 2013).

The kinematics of the head during experimental modeling of an impact or inertial TBI event are described using three-dimensional (3D) linear and angular accelerations along and about the axes of an anatomical coordinate system (ACS), with the origin at, or close to, the head CoM (Namjoshi et al., 2013). In humans and nonhuman primates (NHP), the head ACS is typically based on the Frankfort plane (Hofmann et al., 2016; Nusholtz et al., 1979) from which the location of the origin (corresponding approximately to the head CoM (Yoganandan et al., 2009)) is defined (e.g., Hardy et al., 2007; McIntosh et al., 2014; Nusholtz et al., 1979). In an effort to facilitate better clinical translation, the coordinate systems used to describe human head kinematics in TBI studies should be considered when developing animal models of TBI. Controlled nonimpact impulse exposures to NHPs (with brains that are similar to humans with respect to neuroanatomy and orientation of the neuro-axis) have identified that the direction of rotational brain motion (i.e., the ACS plane in which rotational acceleration is applied) dictates the amount of DAI produced by inertial loading (Abel et al., 1978; Gennarelli et al., 1982, 1987; Margulies et al., 1990). In NHPs, angular accelerations produced by coronal-plane head rotations elicit substantially worse damage to the brain than axial- or sagittal-plane rotations, in extreme cases producing immediate, prolonged coma (Gennarelli et al., 1982). In contrast, when the same exposure type was applied to pigs, axial-plane rotations produced more severe DAI than coronal- or sagittal-plane rotation (Browne et al., 2011; Cullen et al., 2016). This difference may be due to the difference

Significance

This paper describes a method to determine an anatomically relevant coordinate system for the reporting of head kinematics in an ovine model of traumatic brain injury. The locations of the head and brain centers of mass were determined from CT images of 10 sheep skulls. A new anatomical coordinate system is proposed, which better relates to that used for humans. The methods and data provided herein will help the research community to better standardize reporting of the biomechanics of the head in animal models of brain injury, and these may also improve comparisons to human head kinematics descriptions.

in orientation of the spinal-axis relative to the cerebrum (amongst other directional anatomical features) in quadrupedal and bipedal animals (Meaney et al., 1995). These findings demonstrate the importance of species-specific anatomical coordinate systems for defining and describing head kinematics during TBI experiments.

A sheep model of impact acceleration TBI has previously been used (Anderson et al., 2003; Lewis et al., 1996) in which the head is allowed unconstrained motion in six-degrees-of-freedom. In some studies using this model, a head-mounted accelerometer array has been used to measure 3D kinematics during the injury exposure. The acceleration data are transformed from the coordinate system in which they are recorded, to an ACS (ACS_{physical}) formed from the digitization of two external landmarks (notches of the zygomatic processes of the malar bones) and the bregma (intersection of the parietal and frontal bones) which is accessed surgically (Anderson et al., 2003). This ACS_{physical} defines a plane which passes through the brain, but does not represent the natural orientation of the anatomical planes of the sheep head (i.e., equivalent to the Frankfort plane), nor the CoM of the head or brain, the location of which is currently not described in the literature. To our knowledge, there is no anatomically based head coordinate system in sheep or other quadrupedal animals.

The aim of this study was to determine the location of the CoM of the head and brain in Merino wethers, relative to prominent anatomical landmarks, and to define an ACS which has similar orientation to accepted anatomical planes and an origin close to the CoM of the head.

2 | METHODS

2.1 | Study design and CT procedure

Ten male Merino wethers (18–24 months) underwent computed tomography (CT) imaging of the head (Brilliance 16, Philips, USA; 0.37×0.37×0.4mm voxel size). Nine cadaveric sheep heads (decapitated at approximately third cervical vertebrae; obtained via Animal Ethics Committee scavenge approval) were placed in the prone position and underwent CT imaging. One live animal was anesthetized

with intravenous ketamine (0.05 mg/kg; Troy Laboratories Australia, Pty Ltd.) and diazepam (0.04 ml/kg; Ceva Australia), followed by endotracheal intubation and mechanical ventilation (Ohmeda 7000 ventilator, Ohmeda, Madison, WI, USA) delivering 2%–3% isoflurane in a normoxic mix of oxygen [O₂ (30%)] and air (70%) at a flow rate of 4 L/min, and placed in the supine position on the CT scanner bed. This live animal was used under approval of the South Australian Health and Medical Research Institute Animal Ethics Committee (SAM396.19).

2.2 | Generating tissue masks

Image analysis software (MIMICS v22.0, Materialize, USA) was used to determine the head and brain CoM for each animal. Hounsfield unit (HU) threshold bands were used to create initial masks that distinguished the soft tissues (including brain; -150 to 225 HU) and hard tissues (bone and teeth; 226–2,800 HU). As a result of decapitation, the soft tissue mask included material (blood and serous fluid) pooled in the container beneath the head. This fluid layer, in addition to uneven soft tissue of the neck, and the ears, were removed from the model. The ears were excluded because they were inconsistently positioned within the CT scanner, but they were deemed unlikely to substantially affect the head CoM location due to their symmetry (they are typically taped close to the head in these injury models) and low mass. The brain was separated from the refined soft tissue mask using the “split mask” function so that its CoM could be determined independently.

2.3 | Tissue mass and center of mass calculations

The HU associated with each voxel of each tissue mask was exported from MIMICS, and HU values were converted to masses using the relationship described in Equation 1. This scanner-specific calibration equation was derived from scans of density calibration phantoms (Model O62M, Cirs Inc., Norfolk, VA, USA).

$$\rho = 0.625 \times H_{\text{mean}} + 998 \frac{\text{kg}}{\text{m}^3} \quad (1)$$

The volume and total mass of each tissue mask were then determined by summing voxel volume and mass, respectively, using custom MATLAB (R2020a, Mathworks, Natick, MA, USA) code. The x , y , and z coordinates of the CoM (expressed in the CT coordinate system) of each tissue mask were calculated from the CT coordinates (x_{voxel} , y_{voxel} , z_{voxel}) and mass (m_{voxel}) of each voxel, using Equation 2. The mask masses (m_{mask}) and CoM locations were then used to derive the coordinates of the head CoM (x_{head} , y_{head} , z_{head}) (Equation 3).

$$x, y, z_{\text{mask}} = \frac{\sum (x, y, z_{\text{voxel}} \times m_{\text{voxel}})}{\sum m_{\text{voxel}}} \quad (2)$$

$$x, y, z_{\text{head}} = \frac{\sum (x, y, z_{\text{mask}} \times m_{\text{mask}})}{\sum m_{\text{mask}}} \quad (3)$$



FIGURE 1 CoM of the head (black circles: open, each animal; closed, average location) and brain (white circles: open, each animal; closed, average location), relative to the ACS_{physical}, overlaid on bone/teeth and brain masks for a representative animal

2.4 | Development of an ACS with reference to the anatomical planes of sheep head

The head CoM coordinates were imported back into MIMICS and were visualized alongside a 3D model of the hard tissue. Bony landmarks were identified that would produce an ACS (ACS_{virtual}) for which the origin was positioned near the head CoM, and the axes were aligned approximately with the anatomical axes corresponding to the head in a forward-gaze posture (i.e., ovine Frankfort plane equivalent). The coordinates of these anatomical landmarks, and those that defined the previously used sheep head ACS (ACS_{physical}) (Anderson et al., 2003), were identified on the 3D models and exported. In ACS_{physical}, the origin is located at the midpoint between the notches of the left and right zygomatic processes, the x axis is positive toward the notch of the right zygomatic process, the z axis is positive toward the bregma, and the y axis is orthogonal to the x and z axis (Figure 1).

Transformation matrices are required to transform kinematic data from ACS_{physical} to each of the anatomically relevant ACS (ACS_{virtual(Head)} and ACS_{virtual(Brain)}). To compare ACS_{physical} and ACS_{virtual}, the transformation matrix between them was determined for each animal and the difference in orientation between axes was calculated by solving for Euler angles using an x - y - z sequence (Robertson et al., 2013). The translation of the origin was also calculated. The mean transformation matrix from ACS_{physical} to ACS_{virtual} ($T_{\text{physical}}^{\text{virtual}}$) was calculated as follows; the average of each component of the rotation matrices was determined and, using the x - y plane as the reference, cross-products were performed to ensure orthogonality

of the "average" axes (Figure 2). Similar transformation matrices that placed the origin of ACS_{virtual} at the mean CoM location of the head ($T_{\text{physical}}^{\text{head}}$) and brain ($T_{\text{physical}}^{\text{brain}}$) were also determined (Figure 2).

3 | RESULTS

The total head mass was $3,519 \pm 299$ g (mean \pm SD), with mean constituent tissue masses of: brain 155 ± 6 g; bone/teeth 851 ± 75 g; and, soft tissue $2,513 \pm 258$ g (Table 1).

The calculated head CoM was 34.8 ± 3.1 mm from the ACS_{physical} origin, and was positioned anteroinferior to it (Table 2, Figure 1, and Video S1). The brain CoM was 43.7 ± 1.7 mm from the ACS_{physical} origin, and was positioned posterosuperiorly (Table 2, Figure 1, and Video S1).

ACS_{virtual} was defined with the origin at the midpoint between the left and right malar/maxillary junction, the x axis positive toward the notch of the right malar maxillary junction, the z axis positive toward midpoint of the left and right supraorbital foramina, and the y axis orthogonal to the x and z axis. The origin of ACS_{virtual} was, on average, 10.4 ± 3.2 mm from the head CoM (Figure 2, Table 4, Video S2). The brain CoM was, on average, 73.4 ± 5.5 mm from the ACS_{virtual} origin, and remained anteroinferior to it. Relative to ACS_{physical}, the y-z plane was rotated, on average, $-37.5 \pm 2.5^\circ$ about the x axis, providing a more vertical z axis, and an x-y plane parallel to the ground with forward gaze (Table 3). Rotations about the other axes were small (mean $0.3 \pm 0.9^\circ$ about y, $1.2 \pm 1.4^\circ$ about z) (Table 3). The origin was translated as follows: x: 0.2 mm, y: 5.9 mm, and z: -29.4 mm. The complete transformation matrix is provided in Figure 2 and in Supplementary material.

4 | DISCUSSION

Accurate definition of head and brain CoM, and an ACS that facilitates comparison to human head coordinate systems, is needed for

preclinical large animal models of TBI. Such standardized definitions allow rotational and linear accelerations to be defined consistently between animals and between research groups, and increase the potential for comparison with human head TBI kinematics. In this study, the location of head and brain CoMs, relative to a previously reported sheep head ACS (ACS_{physical}), were determined for 10 skeletally mature Merino wethers. A more anatomically representative ACS (ACS_{virtual}), with the origin close to the head CoM and a horizontal plane orientation corresponding approximately with the animal's neutral standing forward-gaze head posture (similar to the human Frankfort plane), was determined using anatomical landmarks defined on CT, and the transformation matrices that place the origin of this ACS at the CoM of the head and brain were calculated.

The estimated brain mass was consistent with that reported previously for Merino sheep (ewes, 160 g) of comparable age and body mass (Lewis et al., 1996). In the present study, the ventricles were included in the brain tissue mask, whereas this comparator harvested brain tissue (Lewis et al., 1996) was likely devoid of cerebrospinal fluid. On average, the brain was 0.24% of body mass, and the head was 5.6% of body mass. The head mass was dominated by the soft tissue (muscle, skin, fat, etc.) components, which comprised, on average, 74.1% of the total head mass.

The ACS_{virtual} origin was, on average, 10 mm from the head CoM, compared to 32 mm for ACS_{physical} (Anderson et al., 2003). Additionally, the ACS_{virtual} axis orientation had better similitude to the typical human head coordinate system, as it resulted an x-y plane corresponding to "forward-gaze" head posture equivalent to the human Frankfort plane. This reorientation would distribute the components of the resultant head kinematics between axes that are more similar to those typically used when reporting for human head kinematics. This could be important because evidence from animal studies (primate and pig) indicates that severity of DAI is dependent on the direction of head rotation (Browne et al., 2011; Cullen et al., 2016; Gennarelli et al., 1982; Ross et al., 1994).

TABLE 1 Body, head, and constituent tissue masses for each animal, estimated from the CT models

Specimen	Body Mass (kg)	Bone/teeth		Brain		Soft tissue		Total	
		Volume (cm ³)	Mass (g)	Volume (cm ³)	Mass (g)	Volume (cm ³)	Mass (g)	Volume (cm ³)	Mass (g)
1	66.5	575.4	845	159.9	163	2,954.1	2,979	3,689.4	3,987
2	69.5	600.3	903	148.6	152	2,423.5	2,455	3,172.4	3,510
3	71.0	531.4	780	154.7	158	2,781.2	2,811	3,467.3	3,748
4	70.5	590.0	861	146.8	150	2,429.4	2,447	3,166.2	3,458
5	68.0	564.3	829	152.8	156	2,362.2	2,389	3,079.3	3,375
6	68.5	648.7	937	153.9	157	2,572.4	2,602	3,375.0	3,696
7	70.5	617.6	919	160.2	164	2,539.3	2,569	3,317.1	3,651
8	68.0	574.9	856	144.9	148	2,349.1	2,377	3,068.9	3,381
9	73.0	605.3	896	155.2	158	2,448.8	2,476	3,209.3	3,530
●10	51.0	460.3	684	143.7	147	2,009.3	2,026	2,613.3	2,857
Mean	67.7	576.8	851	152.1	155	2,486.9	2,513	3,215.8	3,519
SD	6.1	51.8	75	5.9	6	255.3	258	284.9	299

Note: ● = live animal.

TABLE 2 Anatomical coordinates of the CoM for each sheep head and brain, in the ACS_{physical}

Specimen	Head				Brain			
	Center of mass coordinates in landmark ACS _{physical} (mm)			CoM distance to ACS _{physical} origin (mm)	Center of mass coordinates in landmark ACS _{physical} (mm)			CoM distance to ACS _{physical} origin (mm)
x	y	z	x		y	z		
1	0.3	-5.0	-32.1	32.5	-0.6	-16.8	42.3	45.5
2	-1.0	2.7	-37.1	37.3	-0.4	-16.4	38.3	41.6
3	1.7	-4.5	-36.4	36.7	-0.7	-15.1	41.7	44.3
4	1.8	0.8	-33.1	33.2	0.5	-17.9	41.2	44.9
5	-0.4	-3.5	-37.0	37.1	-0.1	-17.7	40.9	44.6
6	1.7	-0.2	-36.0	36.1	0.9	-13.4	40.6	42.7
7	1.0	1.9	-31.6	31.6	-0.9	-11.0	43.1	44.5
8	1.3	-2.5	-38.9	39.0	-0.4	-18.3	41.5	45.4
9	0.8	-1.7	-36.1	36.1	0.1	-11.7	41.8	43.4
● 10	1.5	-0.8	-28.0	28.1	-0.7	-15.1	37.9	39.9
Mean ± SD				34.8 ± 3.1	Mean ± SD			43.7 ± 1.7
Maximum variation from mean				6.7	Maximum variation from mean			3.8

Note: ● = live animal.

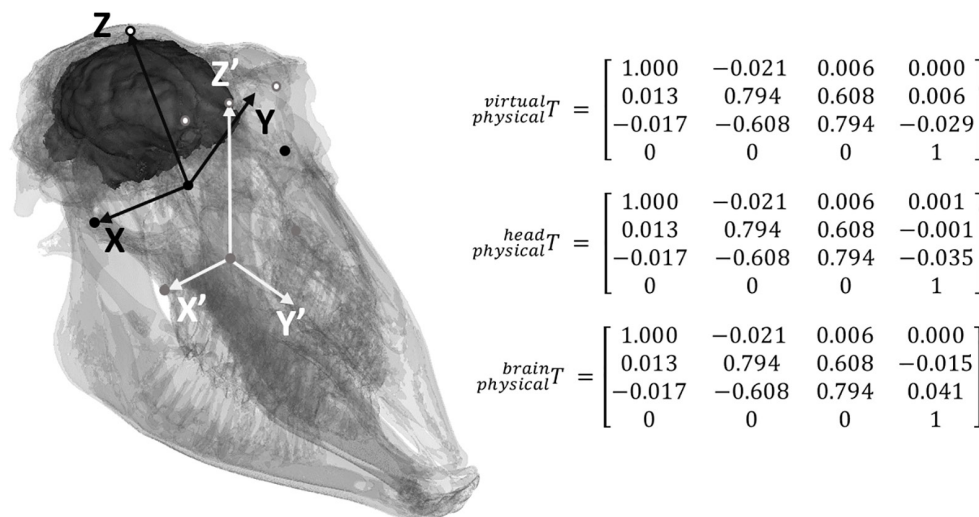


FIGURE 2 ACS_{physical} (black), and ACS_{virtual} (white), with the anatomical landmarks: Left and right malar/maxillary junctions and their midpoint (closed gray circles), left and right supraorbital foramina and their midpoint (open gray circles). The transformation matrices between ACS_{physical} and ACS_{virtual} ($T_{\text{physical}}^{\text{virtual}}$), and between ACS_{physical} and ACS with the origin at the center of mass of the head ($T_{\text{physical}}^{\text{head}}$) and brain ($T_{\text{physical}}^{\text{brain}}$) are shown

Observational studies of human TBI exposure events using video reconstruction methods and/or wearable sensors typically report head kinematics relative to the CoM of the head, which is usually estimated to lie at some standardized distance anterior to the auditory meatus and superior to the Frankfort plane, on the sagittal midline (Slykhouse et al., 2019; Yoganandan et al., 2009). Therefore, describing head kinematics with reference to the CoM of the head and/or brain during exposure events for sheep TBI models, together with application of established acceleration–brain mass scaling relationships (Browne et al., 2011; Holbourn, 1943; Ommaya et al., 1967),

and in the context of other model limitations, may allow better comparison with direction-specific human TBI exposures.

The CoMs of the sheep head and brain were not coincident; the CoM of the head was anterior (rostral) and inferior (ventral) of the brain CoM. Previous TBI research using nonhuman primates has described head accelerations with reference to the CoM of the brain (estimated at the pineal gland, located at the notional “center of the brain”), rather than the head (Abel et al., 1978). The TBI sheep model used by Anderson et al. (2003), used ACS_{physical}, which lies on a plane that passes through the brain, but was not defined with reference

TABLE 3 Angle between ACS_{physical} and ACS_{virtual}, about each axis, for each animal

Specimen	Angle between ACS _{physical} and ACS _{virtual} (about axis in degrees)		
	x	y	z
1	-33.4	0.7	3.8
2	-36.2	1.3	1.8
3	-35.7	0.4	1.1
4	-35.1	1.5	0.8
5	-38.2	-1.1	1.7
6	-36.2	1.1	1.1
7	-38.1	-0.3	1.4
8	-42.2	-1.1	-1.9
9	-39.4	0.1	0.4
● 10	-40.2	0.7	1.9
Mean ± SD	-37.5 ± 2.5	0.3 ± 0.9	1.2 ± 1.4
Maximum variation from mean	4.7	1.4	3.1

Note: ● = live animal.

TABLE 4 Anatomical coordinates of the sheep head CoM and brain CoM, in ACS_{virtual}

Specimen	Head				Brain			
	Center of mass coordinates in ACS _{virtual} (mm)			CoM distance to ACS _{virtual} origin (absolute) (mm)	Center of mass coordinates in ACS _{virtual} (mm)			CoM distance to ACS _{virtual} origin (absolute) (mm)
	x	y	z		x	y	z	
1	-0.9	-13.2	-3.6	13.7	-6.0	-63.8	52.1	82.6
2	-0.7	0.9	-9.3	9.3	-3.0	-59.1	40.3	71.6
3	1.3	-7.2	-9.4	12.0	-2.6	-61.3	47.8	77.8
4	1.3	-0.1	-6.2	6.3	-2.2	-58.1	43.9	72.8
5	-0.2	-3.5	-9.6	10.2	-0.7	-62.8	42.9	76.0
6	0.8	-5.0	-7.9	9.4	-2.1	-60.8	46.2	76.4
7	1.5	-4.2	-4.0	6.0	-1.5	-60.4	46.8	76.4
8	0.5	7.6	-14.8	16.7	2.0	-58.1	34.2	67.4
9	0.1	-1.0	-12.7	12.7	-1.1	-58.1	41.2	71.2
● 10	2.0	0.7	-7.3	7.6	-2.3	-50.6	35.5	61.8
Mean ± SD				10.4 ± 3.2	Mean ± SD			73.4 ± 5.5
Maximum variation from mean				6.3	Maximum variation from mean			11.6

Note: ● = live animal.

to a known CoM of the sheep brain or head. Using the CoM of the brain (instead of the head) as the reference point for describing accelerations associated with exposure events may give rise to better understanding of the relationship between head kinematics and resulting neuropathologies such as DAI. This may be particularly relevant to sheep models of TBI given the distance between the CoM of the head and the CoM of the brain, and this result may extend to other quadrupeds for which the skull cavity housing the brain is not centered in the head due to anterior elongation of the head/snout.

There are several ways in which the data presented herein can be incorporated into TBI animal model protocols (Figure 3), if CT imaging is not available onsite (Generic Pathway), and depending on the extent to which subject-specific models from CT data are defined

(Specimen Specific Pathway A and B). It is often necessary to define landmarks on the animal head and on test equipment (e.g., accelerometers, angular rate sensors, and high-speed tracking markers rigidly mounted on the head; injury apparatus fixed to laboratory floor) in a common laboratory coordinate system to enable accurate definition of the relative position of the anatomy and equipment in space. When the landmarks can be palpated or easily accessed (as for ACS_{physical}), landmark definition can be done using a coordinate measuring machine or motion capture system. However, ACS_{virtual} is based on internal bony landmarks that cannot be physically accessed in vivo. Thus, we propose three potential pipelines to implement the methods and data reported herein to obtain head kinematics at, or close to, the animal's head or brain CoM (Figure 3).

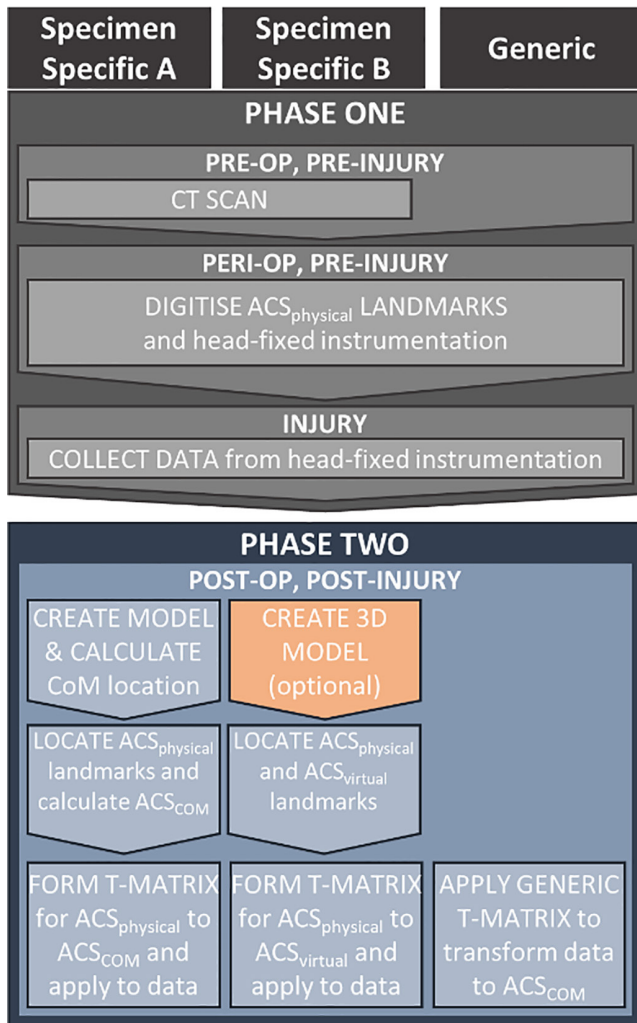


FIGURE 3 Three proposed pathways for implementing the CoM and ACS_{virtual} methods and/or data to produce head kinematics data based on head or brain CoM location/orientation in sheep (or other large animal) TBI models. ACS_{COM} refers to either ACS_{head} or ACS_{brain}, as appropriate for the reference coordinate system

In all cases, the relationship between skull mounted equipment and the skull is determined using the ACS_{physical} landmarks as these are well-defined and can be palpated (zygomatic notch) or accessed via soft tissue resection (bregma). Specimen specific Pathways A and B (Figure 3) require preinjury head CTs. Pathway A is more time and computationally intensive; the CT scans are used to accurately locate CoM of the head and/or brain for each animal, to account for animal-specific anatomical variation. Pathway B uses internal landmarks from the CT, or derived 3D models, to determine ACS_{virtual}. For the Generic pathway, the orientation and origin locations of ACS_{virtual}, ACS_{head}, and ACS_{brain} are estimated by the transformation provided (Figure 2, Supplementary material).

5 | LIMITATIONS

There are several limitations to this study. A validation study of the CT method using the physical tissue was not undertaken. A comparison of

whole head mass would likely have been confounded by the difficulty of accurately physically removing soft tissue similar to that removed virtually in the model. Similar CT modeling methods were previously employed and the outcomes compared to physical measures of CoM for four human cadaveric heads, with no significant difference between the methods detected (Roush, 2010). While most other studies evaluating human head CoM have done so using only physical measurements (as reviewed by (Yoganandan et al., 2009)), some have used CT modeling methods similar to ours (Loyd et al., 2010) and the practice is described briefly elsewhere (Slykhouse et al., 2019). Only skeletally mature Merino wethers were investigated in this study; the head CoM may vary for other sheep species, and by age and sex. Within our specimens, the head CoM varied by approximately 4mm from the mean CoM. Because the majority (9/10) of imaging was performed on decapitated heads from recently deceased animals (~1–3hr), cerebrospinal fluid and blood loss may have occurred, and the tissue was not perfused. This could have affected the morphology of the soft tissues and brain, and therefore the CoM estimations. However, qualitative comparison with the single animal that was scanned in vivo showed no appreciable differences in brain morphology shape or size. Although this animal had lower body mass, and was intubated during the CT scan, the estimated head and brain CoM were comparable to those estimated for the nine ex vivo heads.

6 | CONCLUSIONS

Specimen specific 3D models of sheep head tissues were derived from CT data and used to determine tissue masses and the CoM of both the brain and head. Using these data, an anatomically relevant coordinate system was defined, based on internal landmarks that aligned the head in a neutral (forward gaze) position and with its origin close to the head CoM. The CoMs and ACS_{virtual} defined in this study may allow for better comparison of head kinematics observed in human head trauma exposures with those in ovine TBI models.

ACKNOWLEDGMENTS

The authors acknowledge the facilities and scientific and technical assistance of the National Imaging Facility, a National Collaborative Research Infrastructure (NCRIS) capability, at the Large Animal Research and Imaging Facility (LARIF), South Australian Health and Medical Research Institute (SAHMRI). The authors acknowledge the technical contributions of Manjot Bhatla. Open access publishing facilitated by The University of Adelaide, as part of the Wiley - The University of Adelaide agreement via the Council of Australian University Librarians.

CONFLICT OF INTEREST

The authors declare that there is no conflict of interest.

AUTHOR CONTRIBUTIONS

Conceptualization, CFJ; *Methodology*, JMS, RDQ, CCM and CFJ; *Validation*, JMS, RDQ, CCM and CFJ; *Formal Analysis*, JMS, RDQ

and CCM; *Investigation*, JMS, RDQ, CCM and CFJ; *Resources*, CFJ; *Data Curation*, RDQ; *Writing - Original Draft*, JMS, RDQ, CCM and CFJ; *Writing - Review & Editing*, RDQ and CFJ; *Visualization*, RDQ and CCM; *Supervision*, CFJ; *Project Administration*, CFJ; *Funding Acquisition*, RDQ and CFJ.

PEER REVIEW

The peer review history for this article is available at <https://publons.com/publon/10.1002/jnr.25049>.

DATA AVAILABILITY STATEMENT

The data that support the findings of this study are openly available in Figshare at <https://doi.org/10.25909/c.5929264>.

ORCID

Jessica M. Sharkey  <https://orcid.org/0000-0002-6734-1745>

Ryan D. Quarrington  <https://orcid.org/0000-0002-0633-2482>

Charlie C. Magarey  <https://orcid.org/0000-0002-2974-2409>

Claire F. Jones  <https://orcid.org/0000-0002-0995-1182>

REFERENCES

- Abel, J., Gennarelli, T., & Segawa, H. (1978). Incidence and Severity of Cerebral Concussion in the Rhesus Monkey Following Sagittal Plane Angular Acceleration. SAE Technical Paper 780886. <https://doi.org/10.4271/780886>
- Alshareef, A., Giudice, J. S., Forman, J., Shedd, D. F., Reynier, K. A., Wu, T., Sochor, S., Sochor, M. R., Salzar, R. S., & Panzer, M. B. (2020). Biomechanics of the human brain during dynamic rotation of the head. *Journal of Neurotrauma*, 37(13), 1546–1555.
- Anderson, R. W., Brown, C. J., Blumbergs, P. C., McLean, A., & Jones, N. R. (2003). Impact mechanics and axonal injury in a sheep model. *Journal of Neurotrauma*, 20(10), 961–974.
- Browne, K. D., Chen, X. H., Meaney, D. F., & Smith, D. H. (2011). Mild traumatic brain injury and diffuse axonal injury in swine. *Journal of Neurotrauma*, 28(9), 1747–1755.
- Cullen, D. K., Harris, J. P., Browne, K. D., Wolf, J. A., Duda, J. E., Meaney, D. F., Margulies, S. S., & Smith, D. H. (2016). A porcine model of traumatic brain injury via head rotational acceleration. *Methods in Molecular Biology*, 1462, 289–324.
- Dewan, M. C., Rattani, A., Gupta, S., Baticulon, R. E., Hung, Y. C., Panchak, M., Agrawal, A., Adeleye, A. O., Shrim, M. G., Rubiano, A. M., Rosenfeld, J. V., & Park, K. B. (2019). Estimating the global incidence of traumatic brain injury. *Journal of Neurosurgery*, 130(4), 1080–1097.
- Gennarelli, T. A., Thibault, L. E., Adams, J. H., Graham, D. I., Thompson, C. J., & Marcincin, R. P. (1982). Diffuse axonal injury and traumatic coma in the primate. *Annals of Neurology*, 12(6), 564–574.
- Gennarelli, T. A., Thibault, L., Tomei, G., Wiser, R., Graham, D., & Adams, J. (1987). Directional dependence of axonal brain injury due to centroidal and non-centroidal acceleration. SAE International. <https://doi.org/10.4271/872197>
- Hardy, W. N., Mason, M. J., Foster, C. D., Shah, C. S., Kopacz, J. M., Yang, K. H., King, A. I., Bishop, J., Bey, M., Anderst, W., & Tashman, S. (2007). A study of the response of the human cadaver head to impact. *Stapp Car Crash Journal*, 51, 17–80.
- Hofmann, E., Fimmers, R., Schmid, M., Hirschfelder, U., Detterbeck, A., & Hertrich, K. (2016). Landmarks of the Frankfort horizontal plane: Reliability in a three-dimensional Cartesian coordinate system. *Journal of Orofacial Orthopedics*, 77(5), 373–383. <https://doi.org/10.1007/s00056-016-0045-1>
- Holbourn, A. (1943). Mechanics of head injury. *Lancet*, 242, 438–441.
- Kleiven, S. (2013). Why most traumatic brain injuries are not caused by linear acceleration but skull fractures are. *Frontiers in Bioengineering and Biotechnology*, 1, 15.
- Lewis, S. B., Finnie, J. W., Blumbergs, P. C., Scott, G., Manavis, J., Brown, C., Reilly, P. L., Jones, N. R., & McLean, A. (1996). A head impact model of early axonal injury in the sheep. *Journal of Neurotrauma*, 13(9), 505–514.
- Loyd, A. M., Nightingale, R., Bass, C. R., Mertz, H. J., Frush, D., Daniel, C., Lee, C., Marcus, J. R., Mukundan, S., & Myers, B. S. (2010). Pediatric head contours and inertial properties for ATD design. *Stapp Car Crash Journal*, 54, 167–196.
- Margulies, S. S., Thibault, L. E., & Gennarelli, T. A. (1990). Physical model simulations of brain injury in the primate. *Journal of Biomechanics*, 23(8), 823–836.
- McIntosh, A. S., Patton, D. A., Fréchède, B., Pierré, P. A., Ferry, E., & Barthels, T. (2014). The biomechanics of concussion in unhelmeted football players in Australia: A case-control study. *BMJ Open*, 4(5), e005078.
- Meaney, D. F., Morrison, B., & Dale Bass, C. (2014). The mechanics of traumatic brain injury: A review of what we know and what we need to know for reducing its societal burden. *Journal of Biomechanical Engineering*, 136(2), 021008.
- Meaney, D. F., Smith, D. H., Shreiber, D. I., Bain, A. C., Miller, R. T., Ross, D. T., & Gennarelli, T. A. (1995). Biomechanical analysis of experimental diffuse axonal injury. *Journal of Neurotrauma*, 12(4), 689–694.
- Namjoshi, D. R., Good, C., Cheng, W. H., Panenka, W., Richards, D., Crompton, P. A., & Wellington, C. L. (2013). Towards clinical management of traumatic brain injury: A review of models and mechanisms from a biomechanical perspective. *Disease Models & Mechanisms*, 6(6), 1325–1338.
- Nusholtz, G. S., Melvin, J. W., & Alem, N. M. (1979). Head impact response comparisons of human surrogates. *SAE Transactions*, 88, 3475–3494.
- Ommaya, A., Yarnell, P., Hirsch, A., & Harris, E. (1967). Scaling of experimental data on cerebral concussion in sub-human primates to concussion threshold for man, SAE Technical Paper 670906. <https://doi.org/10.4271/670906>
- Popescu, C., Anghelescu, A., Daia, C., & Onose, G. (2015). Actual data on epidemiological evolution and prevention endeavours regarding traumatic brain injury. *Journal of Medicine and Life*, 8(3), 272–277.
- Robertson, D. G. E., Caldwell, G. E., Hamill, J., Kamen, G., & Whittlesey, S. (2013). *Research methods in biomechanics* (2nd ed.). Human Kinematics.
- Ross, D. T., Meaney, D. F., Sabol, M. K., Smith, D. H., & Gennarelli, T. A. (1994). Distribution of forebrain diffuse axonal injury following inertial closed head injury in miniature swine. *Experimental Neurology*, 126(2), 291–299.
- Roush, G. C. (2010). Finding cadaveric human head masses and center of gravity: A comparison of direct measurement to 3D ing. Wright State University.
- Slykhouse, L., Zaseck, L. W., Miller, C., Humm, J. R., Alai, A., Kang, Y. S., Dooley, C., Sherman, D., Bigler, B., Demetropoulos, C. K., Reed, M. P., & Rupp, J. D. (2019). Anatomically-based skeletal coordinate systems for use with impact biomechanics data intended for anthropomorphic test device development. *Journal of Biomechanics*, 92, 162–168.
- Smith, D. H., Chen, X. H., Xu, B. N., McIntosh, T. K., Gennarelli, T. A., & Meaney, D. F. (1997). Characterization of diffuse axonal pathology and selective hippocampal damage following inertial brain trauma in the pig. *Journal of Neuropathology and Experimental Neurology*, 56(7), 822–834.
- Smith, D. H., Meaney, D. F., & Shull, W. H. (2003). Diffuse axonal injury in head trauma. *The Journal of Head Trauma Rehabilitation*, 18(4), 307–316.
- Ueno, K., & Melvin, J. W. (1995). Finite element model study of head impact based on hybrid III head acceleration: The effects of rotational and translational acceleration. *Journal of Biomechanical Engineering*, 117(3), 319–328.

- Yoganandan, N., Pintar, F. A., Zhang, J., & Baisden, J. L. (2009). Physical properties of the human head: Mass, center of gravity and moment of inertia. *Journal of Biomechanics*, *42*(9), 1177–1192.
- Zuckerman, S. L., Reynolds, B. B., Yengo-Kahn, A. M., Kuhn, A. W., Chadwell, J. T., Goodale, S. E., Lafferty, C. E., Langford, K. T., McKeithan, L. J., Kirby, P., & Solomon, G. S. (2018). A football helmet prototype that reduces linear and rotational acceleration with the addition of an outer shell. *Journal of Neurosurgery*, *130*(5), 1634–1641.

How to cite this article: Sharkey, J. M., Quarrington, R. D., Magarey, C. C. & Jones, C. F. (2022). Center of mass and anatomical coordinate system definition for sheep head kinematics, with application to ovine models of traumatic brain injury. *Journal of Neuroscience Research*, *100*, 1413–1421. <https://doi.org/10.1002/jnr.25049>

SUPPORTING INFORMATION

Additional supporting information may be found in the online version of the article at the publisher's website.

Video S1

Video S2

Supplementary material

Supplementary material